Vercher Martínez, A.; Giner Maravilla, E.; Arango Villegas, C.; Tarancón Caro, JE.; Fuenmayor Fernández, FJ. (2014). Homogenized stiffness matrices for mineralized collagen fibrils and lamellar bone using unit cell finite element models. Biomechanics and Modeling in Mechanobiology. 13(2):1-21. doi:10.1007/s10237-013-0507-y.

Noname manuscript No.
(will be inserted by the editor)

Homogenized stiffness matrices for mineralized collagen fibrils and lamellar bone using unit cell finite element models

Ana Vercher · Eugenio Giner · Camila Arango · José E. Tarancón · F. Javier Fuenmayor

Received: date / Accepted: date

Abstract Mineralized collagen fibrils have been usually analyzed like a two phase composite material where crystals are considered as platelets that constitute the reinforcement phase. Different models have been used to describe the elastic behavior of the material. In this work, it is shown that, when Halpin-Tsai equations are applied to estimate elastic constants from typical constituent properties, not all crystal dimensions yield a model that satisfy thermodynamic restrictions. We provide the ranges of platelet dimensions that lead to positive definite stiffness matrices. On the other hand, a finite element

A. Vercher (✉) · E. Giner · C. Arango · J.E. Tarancón · F.J. Fuenmayor
Centro de Investigación de Tecnología de Vehículos - CITV,
Depto. de Ingeniería Mecánica y de Materiales,
Universitat Politècnica de València, Camino de Vera, 46022 Valencia, Spain
E-mail: anvermar@dimm.upv.es

model of a mineralized collagen fibril unit cell under periodic boundary conditions is analyzed. By applying six canonical load cases, homogenized stiffness matrices are numerically calculated. Results show a monoclinic behavior of the mineralized collagen fibril. In addition, a 5-layer lamellar structure is also considered where crystals rotate in adjacent layers of a lamella. The stiffness matrix of each layer is calculated applying Lekhnitskii transformations and a new finite element model under periodic boundary conditions is analyzed to calculate the homogenized 3D anisotropic stiffness matrix of a unit cell of lamellar bone. Results are compared with the rule-of-mixtures showing in general good agreement.

Keywords Mineralized collagen fibril · Lamellar bone · Cortical bone · Finite elements · Periodic boundary conditions · Homogenized stiffness matrix

1 INTRODUCTION

When cortical bone matures, its first woven structure becomes a parallel fibred bone and finally a lamellar bone (Cowin, 2001). The main unit of lamellar bone is the lamella of about 3-7 μm thick (Rho et al., 1998). A lamella is composed of mineralized collagen fibrils embedded in a mineralized extra-fibrilar matrix. It is well known that the collagen fibrils orientation pattern in the lamella is an important feature because mechanical properties depend on bone structure at the very small scale. In 1906, Gebhardt observed that collagen fibrils are unidirectionally oriented in each lamella, changing suddenly their orientation between adjacent lamella. Later, Ascenzi and Bonucci (Ascenzi and Bonucci,

1967, 1968) held the idea of an unidirectional collagen fibril orientation in each lamella, basing their results on polarized light microscopy (PLM) images of secondary osteons. Subsequently, Wagner and Weiner (1992) also suggested a unidirectional fibril orientation in each lamella. These authors calculated elastic constants of an individual lamella by using several composite material models (Padawer and Beecher, 1970; Lusis et al., 1973; Halpin, 1984). It seems that the first investigators who analyzed a lamella as a two-phase composite material were Currey (1962) and Bondfield and Li (1967). More recent investigations consider a lamella as a layered structure where a collagen fibril orientation pattern exists (Giraud-Guille, 1988; Akiva et al., 1998; Weiner et al., 1999; Wagermaier et al., 2006). The orientation of collagen fibrils changes in successive layers. Reisinger et al. (2011) develop a detailed analysis of elastic properties of the microstructure using a finite element model in which the elastic constants of lamellar bone have been calculated using homogenization theories in a previous work (Reisinger et al., 2010). These authors analyze several collagen fibril orientation patterns. They conclude that the model proposed by Weiner et al. (1999), based on a 5-layered structure in an individual lamella, is in good agreement with experimental results. In the work of Martínez-Reina et al. (2011), a complete analytical model of the lamellar bone is developed to calculate elastic properties of bone.

At a smaller scale, mineralized collagen fibrils are the basic building block of the lamellae (Weiner and Wagner, 1998). Collagen type I and carbonate apatite crystals are the basic constituents of mineralized collagen fibrils. Several

works have been developed to calculate elastic constants of mineralized collagen fibrils. In Reisinger et al. (2010), homogenization theory of Mori Tanaka is used to estimate elastic properties of mineralized collagen fibrils. However, they suppose that the crystals are spheroidal and randomly distributed. Yuan et al. (2011) calculate the elastic modulus of mineralized collagen fibrils by finite elements supposing a concentric arrangement of minerals around fibril axes. In the work of Martínez-Reina et al. (2011), elastic constants of mineralized collagen fibrils are also estimated considering water presence.

In this work, we provide estimations of the 3D stiffness matrices and elastic constants both at the mineralized collagen fibril scale and at the lamellar scale using numerical finite element models. The first numerical model is based on a representative unit cell of a mineralized collagen fibril, composed of a collagen matrix and apatite crystals arranged as staggered platelets. The results at the fibril level are then used at the lamellar scale, performing a second finite element model for the lamellar bone. In this case, the representative unit cell consists of five layers in which the fibrils are arranged in different directions with respect to the osteon axis. In this model, the rotation of the platelets within the fibrils is also taken into account. It is shown that this rotation angle has an important influence on the elastic behavior, which in general is highly anisotropic.

In this study, the reinforcement phase is modelled as platelets distributed in a staggered arrangement in the axial direction of the fibril and in parallel layers in the transverse direction of the fibril. To the authors' knowledge, a 3D

finite element model of this type has not yet been reported in the literature. In addition, we show that Halpin-Tsai equations cannot be used for all the dimensions of apatite crystals measured experimentally by Rubin et al. (2003), because the thermodynamic restrictions are not fulfilled in all cases for typical constituent properties found in the literature. We have carried out a detailed analysis for the different aspect ratios, providing crystal dimension ranges that satisfy these restrictions when Halpin-Tsai equations are used.

The article is organized as follows. In Section 2, the elastic constants of mineralized collagen fibrils are reviewed in the context of composite material models and Halpin-Tsai equations are summarized. When the mineralized collagen fibril direction changes, Lekhnitskii transformations are used to calculate the elastic constants in the osteon axes directions (Akiva et al., 1998). The thermodynamic restrictions are included in order to ensure that the orthotropic stiffness matrix is positive definite. In Section 3 a finite element model of a mineralized collagen fibril unit cell subjected to periodic boundary conditions (PBCs) is detailed to calculate the homogenized stiffness matrix by applying six canonical load cases. In Section 4, we review the fibril orientation pattern of a 5-layer lamellar structure proposed by Weiner et al. (1999) and we present the corresponding finite element model under PBCs for the lamellar unit cell. Results are detailed in Section 5. It is found that a monoclinic homogenized 3D stiffness matrix for mineralized collagen fibrils is obtained in contrast to previous proposals that yield orthotropic behavior. Next, the anisotropic homogenized 3D stiffness matrix of lamellar bone is calculated

and the elastic constants are compared with the ones obtained using the rule-of-mixtures. Finally, the most important conclusions of this work are discussed in Section 6.

2 ELASTIC CONSTANTS OF MINERALIZED COLLAGEN FIBRILS

2.1 Analytical model based on Halpin-Tsai and Lekhnitskii transformation

The bibliography about elastic properties of platelet or ribbon reinforced composites is scarce. In the works of Wagner and Weiner (1992) and Akiva et al. (1998) different models are explained in detail. According to Halpin and Tsai, the following equations are used to calculate certain elastic constants (Halpin, 1984):

$$\frac{\bar{p}}{p_m} = \frac{(1+\zeta\eta V_f)}{(1-\eta V_f)} \qquad ; \qquad \eta = \frac{(p_f/p_m - 1)}{(p_f/p_m + \zeta)} \tag{1}$$

where $\bar{p}$ is the composite property (E_{11}, E_{22}, G_{12}, G_{23}, ν_{12}, ν_{23}), p_f and p_m are the constituent properties, i.e. the reinforcement and matrix properties, respectively, V_f is the volume fraction of platelet reinforcement and ζ represents a factor function of the geometry of the reinforcement, packing geometry and loading conditions. Subscripts $1, 2, 3$ are the directions of the local orientated coordinate system shown in Fig. 1. The volume fraction of platelet reinforcement V_f is given by:

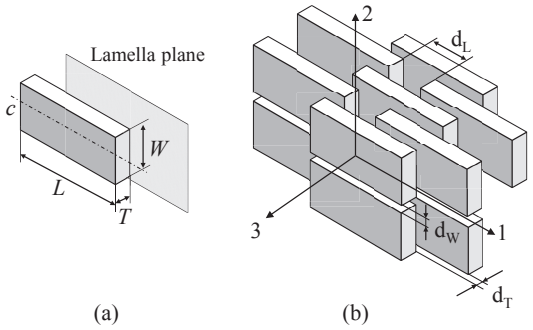

Fig. 1 (a) Crystal dimensions L, W, T and the principal axis of the crystal, c. (b) Schematic staggered crystal arrangement, showing the definition of the local orientated coordinate system $(1, 2, 3)$. d_L, d_W and d_T are the distances between adjacent crystals

$$V_f = \frac{LWT}{(L + d_L)(W + d_W)(T + d_T)} \tag{2}$$

where L is the platelet length, W is the platelet width, T is its thickness and d_L, d_W and d_T are the longitudinal, transverse in-plane and transverse out-of-plane distances between platelets, respectively, see Fig. 1.

Halpin did not provide expressions to calculate ζ for the out-of-plane Young's modulus, E_{33}, shear modulus, G_{31}, and Poisson's ratio, ν_{31}, so in this work, it is assumed that $\zeta_{E_{33}} = 2T/(L + W)$, $\zeta_{G_{31}} = \zeta_{G_{23}}$ and $\zeta_{\nu_{31}} = \zeta_{\nu_{23}}$ following Akiva et al. (1998).

In this context, the elastic compliance matrix $\mathbf{S}^l$ for an orthotropic material expressed in an orientated coordinate system $(1, 2, 3)$, see Fig. 1, can be calculated (Gibson, 1994) and, therefore, the orthotropic stiffness matrix $\mathbf{C}^l = \left(\mathbf{S}^l\right)^{-1}$. Superscript l denotes the local coordinate system.

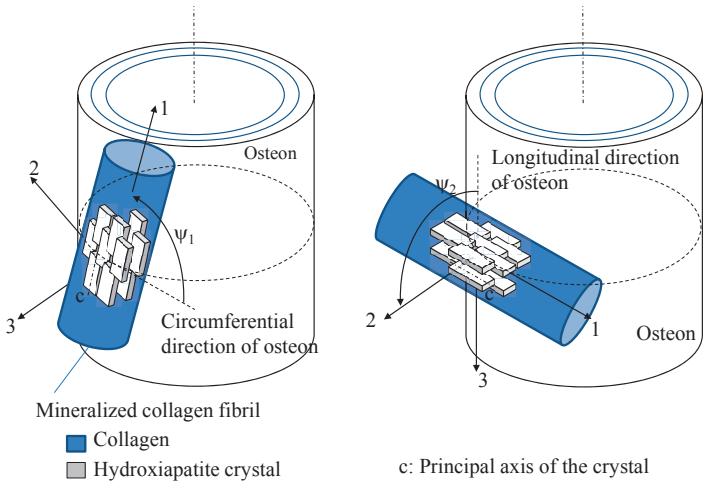

Fig. 2 Schematic representation of the two possible rotations ψ_1 and ψ_2 considered. Coordinate system $1, 2, 3$ is solidary with the mineralized collagen fibril

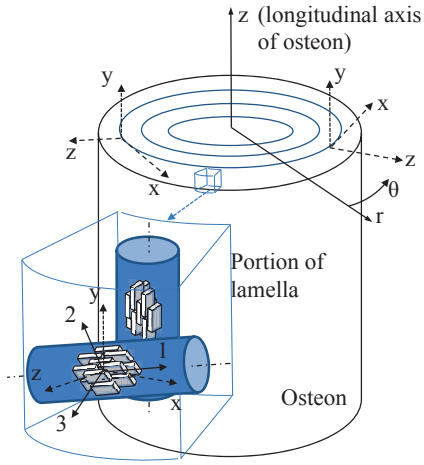

Fig. 3 Coordinate system scheme: cylindrical coordinate system (r, θ, z) is used as a global coordinate system and a local auxiliary coordinate system (x, y, z) is defined at any point, being (x, y, z) coincident with (θ, z, r) respectively

Table 1 *Cosines of the angles that the local auxiliary directions* (x, y, z) *form with respect to the local orientated directions* $(1, 2, 3)$

	1	2	3
x	α_1	β_1	γ_1
y	α_2	β_2	γ_2
z	α_3	β_3	γ_3

$\alpha_1 = \cos(\psi_1)$ $\quad \beta_1 = \sin(\psi_1)\cos(\psi_2)$ $\quad \gamma_1 = -\sin(\psi_1)\sin(\psi_2)$

$\alpha_2 = -\sin(\psi_1)$ $\quad \beta_2 = \cos(\psi_1)\cos(\psi_2)$ $\quad \gamma_2 = -\cos(\psi_1)\sin(\psi_2)$

$\alpha_3 = 0$ $\quad \beta_3 = \sin(\psi_2)$ $\quad \gamma_3 = \cos(\psi_2)$

In addition, Fig. 2 shows two possible rotations of the crystals. First, the crystal can rotate an angle ψ_1 about the radial axis. Second, the apatite crystal can rotate an angle ψ_2 about its own axis, c. The principal axis of the crystals, c which is coincident with axis 1, always remains parallel to the lamella tangential plane.

On the other hand, a cylindrical coordinate system associated with the osteon, (r, θ, z) is defined, see Fig. 3. In addition, a local auxiliary coordinate system (x, y, z) at any point can be defined, whose axes can be identified with the directions θ, z, r, respectively of the cylindrical coordinate system at that point. The compliance matrix of a mineralized fibril expressed in the local auxiliary coordinate system (x, y, z), can be calculated using the Lekhnitskii transformation (Lekhnitskii, 1963). Table 1 defines the cosines of the angles between the two coordinate systems. In this work, the expressions proposed by Akiva et al. (1998) are used. The stiffness matrix of a mineralized collagen fibril, with a general orientation in the osteon or global coordinate system (r, θ, z), $\mathbf{C}^g$, will present a full form.

2.2 Thermodynamic restrictions

In order to fulfill thermodynamic principles, the compliance and stiffness matrices have to be positive definite, see e.g. Gurtin (1972). Hence, this condition implies that the elastic constants of the stiffness matrix have to verify some relations. Lempriere (1968) expressed these relations for an orthotropic material as follows:

$$E_{11}, E_{22}, E_{33}, G_{23}, G_{31}, G_{12} > 0 \tag{3}$$

$$|\nu_{21}| < \left(\frac{E_{22}}{E_{11}}\right)^{0.5} \quad |\nu_{12}| < \left(\frac{E_{11}}{E_{22}}\right)^{0.5} \tag{4}$$

$$|\nu_{13}| < \left(\frac{E_{11}}{E_{33}}\right)^{0.5} \quad |\nu_{31}| < \left(\frac{E_{33}}{E_{11}}\right)^{0.5} \tag{5}$$

$$|\nu_{23}| < \left(\frac{E_{22}}{E_{33}}\right)^{0.5} \quad |\nu_{32}| < \left(\frac{E_{33}}{E_{22}}\right)^{0.5} \tag{6}$$

$$1 - \nu_{21}\nu_{12} - \nu_{13}\nu_{31} - \nu_{32}\nu_{23} - 2\nu_{12}\nu_{31}\nu_{23} > 0 \tag{7}$$

$$1 - \nu_{13}\nu_{31} > 0 \tag{8}$$

$$1 - \nu_{21}\nu_{12} > 0 \tag{9}$$

$$1 - \nu_{32}\nu_{23} > 0 \tag{10}$$

$$\nu_{21}\nu_{32}\nu_{13} < \frac{1 - \nu_{21}^2\left(\frac{E_{11}}{E_{22}}\right) - \nu_{32}^2\left(\frac{E_{22}}{E_{33}}\right) - \nu_{13}^2\left(\frac{E_{33}}{E_{11}}\right)}{2} < \frac{1}{2} \tag{11}$$

In the technical note of Cowin and van Buskirk (1986) these thermodynamic restrictions are summarized and they were used to verify the elastic constants of bone obtained by Ashman et al. (1984) through ultrasound techniques.

3 MINERALIZED COLLAGEN FIBRIL: UNIT CELL FINITE ELEMENT MODEL

3.1 Unit cell under periodic boundary conditions

A unit cell model can be used to estimate the behavior of an heterogeneous material (Suquet, 1987; Hohe, 2003; Pahr and Rammerstofer, 2006). If periodic boundary conditions are considered, the response of the unit cell will be representative of the whole structure. Following Reisinger et al. (2011), periodic boundary conditions must fulfill two conditions: the stress field must be periodic, $\sigma_{ij}^{+} = \sigma_{ij}^{-}$, and the deformed shape of opposite sides of the unit cell must be identical. This way, a strain-periodic displacement field is attained.

Six independent unitary strain fields are applied in order to obtain the corresponding column i of the stiffness matrix, $\mathbf{C}_{:,\mathrm{i}}$.

The Lamé-Hooke constitutive equation, is given by:

$$\boldsymbol{\sigma} = \mathbf{C}\boldsymbol{\epsilon} \tag{12}$$

where $\boldsymbol{\sigma} = (\sigma_{xx} \;\; \sigma_{yy} \;\; \sigma_{zz} \;\; \tau_{yz} \;\; \tau_{zx} \;\; \tau_{xy})^{\mathrm{T}}$ is the stress vector, $\mathbf{C}$ is the stiffness matrix and $\boldsymbol{\epsilon} = (\epsilon_{xx} \;\; \epsilon_{yy} \;\; \epsilon_{zz} \;\; \gamma_{yz} \;\; \gamma_{zx} \;\; \gamma_{xy})^{\mathrm{T}}$ is the strain vector imposed, i.e.:

Load case 1: $\boldsymbol{\epsilon}^1 = (1 \;\; 0 \;\; 0 \;\; 0 \;\; 0 \;\; 0)^{\mathrm{T}}$, then $\mathbf{C}_{:,1} = \boldsymbol{\sigma}^1$ ...

Load case 6: $\boldsymbol{\epsilon}^6 = (0 \;\; 0 \;\; 0 \;\; 0 \;\; 0 \;\; 1)^{\mathrm{T}}$, then $\mathbf{C}_{:,6} = \boldsymbol{\sigma}^6$

where $\boldsymbol{\sigma}^i$ is the equilibrium stress vector corresponding to the strain field $\boldsymbol{\epsilon}^i$. Stress components are obtained from the finite element results.

In order to apply periodic boundary conditions to ensure that the hexahedron analyzed is a representative volume of the entire domain, displacement gradients along the corresponding external surface must be equal. In this work, equations proposed by Hohe (2003) are used. In addition, it is necessary to fully constrain the model to avoid rigid solid motions and, therefore, the central node of the finite element model is constrained.

The analysis has been performed with the finite element commercial code Ansys^{TM}. The equation set has been applied with the command `Constraint Equation`. A macro has been developed to apply constraint equations due to the large number of constraints.

3.2 Mineralized collagen fibrils

Mineralized collagen fibrils are the building blocks of the lamellae. One of the principal constituents of the fibril is collagen type I arranged in the triple-helical molecule. Collagen molecules are staggered in the axial direction of the fibril by a periodic distance of $D = 67$ nm, as commonly accepted in the literature, and the length of the collagen molecule is approximately $4.4D = 294.8$ nm (Rho et al., 1998; Orgel et al., 2001).

The crystals are the other principal component of the mineralized collagen fibrils. They are platelet-shaped and a wide range of dimensions has been reported in the literature: 15-150 nm in length, 10-80 nm in width and 2-7 nm in thickness (Rubin et al., 2003). Distance between the platelets is of the same order as the crystal thickness, between 2 and 4.5 nm and volume

fraction between 30% and 48% (Lowenstam et al., 1989). There exist other non-collagenous proteins but their volume fraction is lower than 10% (Yuan et al., 2011).

It seems clear that mineral platelets follow a staggered arrangement in the axial direction of the collagen fibril (Hassenkam et al., 2004; Jäger and Fratz, 2000; Orgel et al., 2001; Rubin et al., 2003). However, the arrangement pattern of mineral platelets in the radial (or transverse) direction of the fibril is still not well known (Yuan et al., 2011). For many investigators, crystals organization in mineralized collagen fibrils is considered as a structure of parallel layers that traverse the fibril (Weiner et al., 1999; Landis et al., 1996; Erts et al., 1994; Weiner and Wagner, 1998). Nevertheless, Yuan et al. (2011) consider that the crystal arrangement in parallel layers inside the fibril is only true at a small scale. At a large scale, collagen molecules are assembled in a concentric pattern (Hulmes et al., 1995) so the mineral platelets will grow in a concentric arrangement (Jäger and Fratz, 2000) in the fibril. The staggered mineral arrangement has been widely reviewed by Ji and Gao (2004). In several works (Zuo and Wei, 2007; Zhang et al., 2010), the mechanical properties of bone-like hierarchical materials, based on a staggered mineral arrangement, are studied. In the recent work of Bar-On and Wagner (2012) an analytical expression for the effective modulus along the stagger direction is formulated, although a different basic unit cell is considered. In the work here presented, mineral platelets are supposed to be arranged in parallel layers that traverse

the fibril following Rho et al. (1998), Weiner and Wagner (1998) and Weiner et al. (1999).

3.3 Finite element model

In our finite element model of a mineralized collagen fibril, mineral crystals are modelled as platelets of dimensions $L \times W \times T$. A periodic solid model of the staggered pattern that crystals follow in axial direction can be seen in Fig. 4 for three volume fraction values ($V_f = 0.1$, $V_f = 0.3$ and $V_f = 0.45$). In order to perform the analysis, a unit cell $a \times b \times c$ has been modelled fixing the boundaries compatible with geometrical periodicity. The 3D model has been meshed with linear solid hexahedra. In Fig. 5 a detail of the numerical model is shown.

Because there are many variables that could be considered for a given volume fraction, in this work some of them are fixed, as frequent values, $T = 5$ nm, $W = 30$ nm and the space between crystals $d_W = d_T = 2$ nm. The distance between crystals in the longitudinal axis, d_L, is calculated as $d_L = 4.4D - L$ because the periodical unit in this direction must be equal to the molecule length. Therefore, L is calculated through Eq. (2) for every volume fraction. Note that a periodical model in transverse direction takes place for each five molecules in the longitudinal direction. Considering these crystal dimensions and their periodic arrangement, the dimensions of the hexahedral representative volume shown in Fig. 4 are $a = 4.4D = 294.8$ nm, $b = 32$ nm and $c = 154$ nm.

Although $V_f = 0.1$ is not a usual volume fraction in bone, it is considered here to evaluate the influence of collagen compliance on the mineralized collagen fibril stiffness when no mineral gaps occur. In the case of $V_f = 0.45$, the crystal length L tends to be very large.

Certainly, mineral crystals not only nucleate at gaps of collagen molecules but they are also deposited along the molecule length. These crystals together with non-collagenous proteins form the extra-fibrillar matrix where fibrils are embedded. In this work the presence of the mineralized extra-fibrillar matrix is not explicitly considered but the mineral volume fraction in the fibril, $V_f = 0.3$, can be used as a representative value of the total mineral content in both fibril and extra-fibrillar matrix (Reisinger et al., 2011).

4 LAMELLAR BONE: ELASTIC CONSTANTS AND UNIT CELL FINITE ELEMENT MODEL

4.1 Fibril orientation pattern

In this work, the fibril orientation pattern proposed by Weiner et al. (1999) is considered. These authors base their study on several TEM and SEM micrographies arriving at the conclusion that a lamellar unit is an asymmetric structure formed by five sub-layers in which fibrils change their orientation. These authors infer from several studies that the variation of the sublayer thickness is directly related to the strength capabilities of the bone.

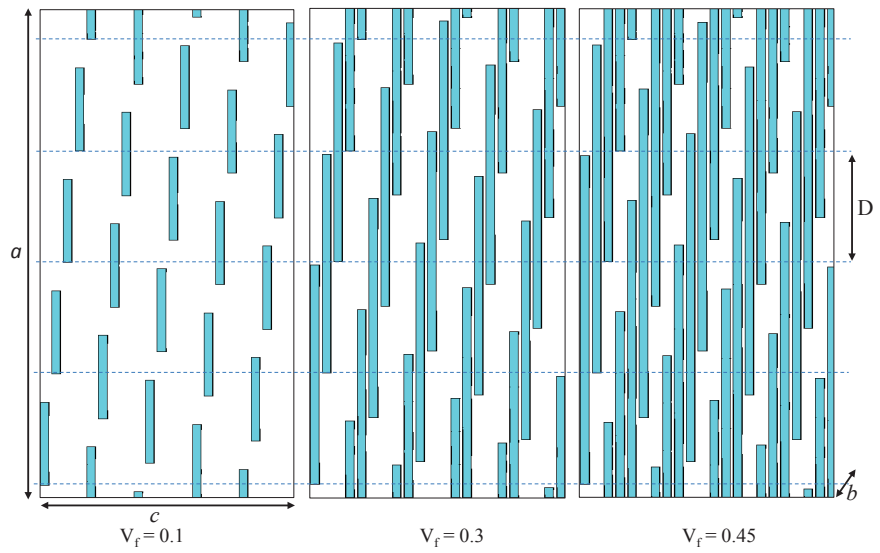

Fig. 4 (a) Staggered arrangement of crystals in the mineralized collagen fibril (proportions are preserved) for different volume fractions. Boundaries of the unit cell ($a \times b \times c$) are marked. D is the periodic distance equal to 67 nm

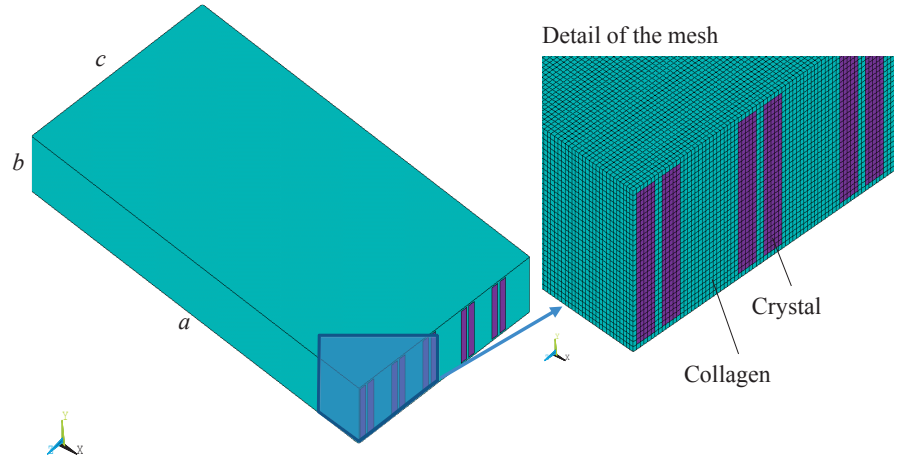

Fig. 5 Solid model and detail of the finite element model of mineralized collagen fibril, $V_f = 0.3$

In the work of Weiner et al. (1999), the successive sublayers forming a lamellar unit are rotated approximately 30° between them (see Fig. 6). In the sublayer at 0° (sublayer 1 in Fig. 6), the crystal layer is parallel to the boundary plane of the lamellar unit. Here the c-axes (which are parallel to the local orientated axis 1) of the crystals are transversely arranged with respect to the longitudinal osteon axis. This sublayer corresponds to the thin layer and its about 0.4 μm thick (Akiva et al., 1998). In the successive sublayers the c-axes of the crystals rotate an angle ψ_1=(30°, 60°, 90°, 120°). The rotation angle ψ_2 (the crystal rotation around its own c-axis) is not well known (Akiva et al., 1998). Second and third sublayers constitute a transition zone of about 0.4 μm in thickness. In the work of Akiva et al. (1998), the fourth and fifth layers are named thick and back-flip layers and are about 1.8 μm and 0.6 μm thick respectively. This pattern can be seen as a rotated plywood structure.

The recent work of Faingold et al. (2012) presents a nanoindentation study of individual osteon lamella in order to understand the microstructural arrangement of the mineralized collagen fibrils and the hydroxiapatite platelet orientation. They conclude that lamellae exhibit different behavior, from the inner to the outer in the osteonal radial direction, especially the first lamella (the closest to the Havers' canal). Their results are in agreement with the rotated plywood arrangement of the mineralized fibrils. In the study of Rezkinov et al. (2013) a different structure of lamellar bone is presented. These authors analyze the circumferential lamellar bone located in the periosteal region of

rat tibia. They conclude that there are three kinds of sub-layers having one of them a rotated plywood structure.

4.2 Analytical model based on the rule-of-mixtures

Once the elastic constants of the sublayers forming a lamellar unit are determined, a first approximation to the elastic constants of lamellar bone can be obtained using the rule-of-mixtures (Wagner and Weiner, 1992; Akiva et al., 1998) as follows:

$$D_{lam} = \frac{1}{T}(T_1 D_1 + T_2 D_2 + T_3 D_3 + T_4 D_4 + T_5 D_5) \tag{13}$$

where T_i is the thickness of the sublayer i and T is the lamellar unit thickness, $T = \sum T_i$, with $i = 1...6$. D_{lam} is the elastic property of the lamella and D_i is the corresponding elastic property of each sublayer.

4.3 Finite element model

In this case, the unit cell is divided into five volumes corresponding to the five sublayers described in Section 4.1. The stiffness matrix of each sublayer has previously been calculated using the finite element model of a mineralized collagen fibril as described in Section 3 and the Lekhnitskii transformation (Section 2.1), to consider the mineralized collagen fibrils rotations, ψ_1 and ψ_2 (see Fig. 2). The variables in the model are: the angle that the *c*-axis rotates between sublayers, ψ_1=$(0°, 30°, 60°, 90°, 120°)$, and the angle that the crystal

rotates about its own axis ψ_2. The angle ψ_2 is 0° from the first to the third sublayers and several combinations of ψ_2 are considered for the fourth and the fifth sublayers, i.e.: $(0^\circ, 0^\circ), (50^\circ, 90^\circ), (70^\circ, 90^\circ), (70^\circ, 30^\circ)$, respectively. Sublayer thicknesses are assumed to be $t = (0.4, 0.2, 0.2, 1.8, 0.6)$ μm (Akiva et al., 1998).

In Fig. 6, the finite element model is shown together with a schematic illustration of how mineralized collagen fibrils change their orientation in the successive five sublayers. Volumes corresponding to each sublayer are numbered from 1 to 5. Note that sublayer 1 is divided into two portions in the model in order to satisfy a continuum periodical stress field.

Following the same procedure described in Section 3, periodic boundary conditions and six independent unitary strain fields are applied. Then, the anisotropic stiffness matrix of the lamellar unit can be calculated.

5 RESULTS

5.1 Range of mineral aspect ratios compatible with thermodynamic restrictions using Halpin-Tsai equations

As mentioned above a wide range of crystal platelets dimensions can be found in the bibliography: $L = 15 - 150$ nm, $W = 10 - 80$ nm and $T = 2 - 7$ nm (Rubin et al. 2003). When Halpin-Tsai equations are used to estimate theoretically elastic constants of a mineralized collagen fibril for typical constituent properties (Wagner and Weiner, 1992; Akiva et al., 1998), one should pay at-

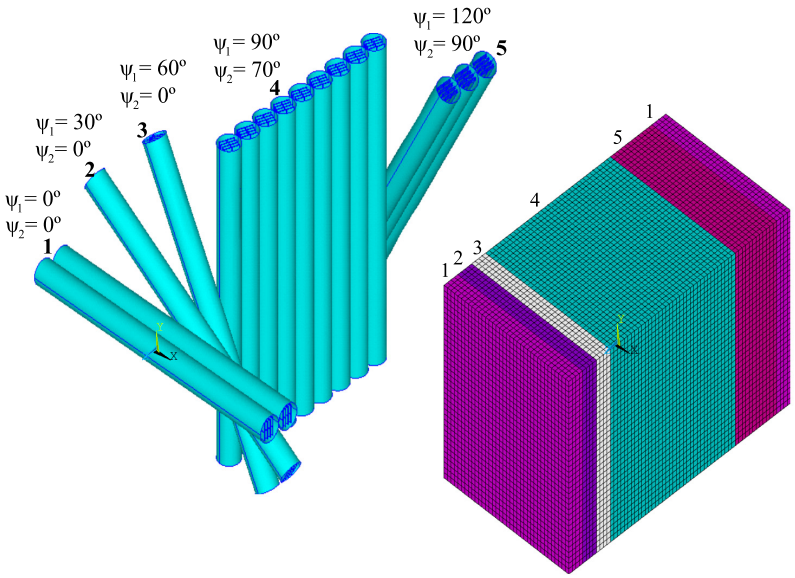

Fig. 6 Finite element model of a representative unit lamellar cell and schematic illustration of the five sublayers proposed by Weiner et al. (1999)

tention to the values of crystal aspect ratios, L/T and W/T, because not all the possible crystal aspect ratios verify the thermodynamical restriction summarized in Section 2.2. In what follows a detailed study of the influence of the aspect ratios on the elastic constants is presented for Halpin-Tsai equations, and the range of aspect ratios that fulfill the thermodynamic restrictions is provided. This study has been performed using the collagen and apatite elastic properties provided by Akiva et al. (1998), i.e. $E_{col} = 1.5$GPa, $E_{ap} = 114$GPa, $\nu_{col} = 0.38$, $\nu_{ap} = 0.3$. These values are similar to those found in other works, e.g. Martínez-Reina et al. (2011). In addition, we also consider a volume fraction of 0.5 as in Akiva et al. (1998).

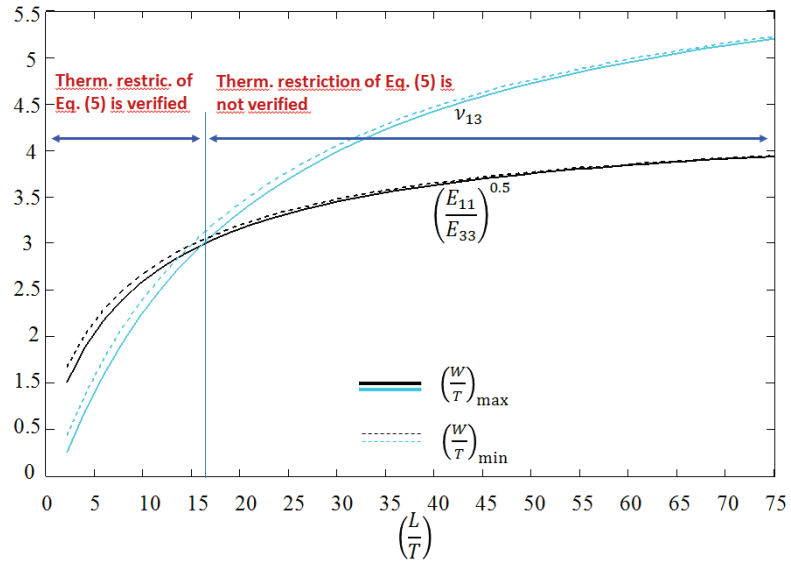

Fig. 7 Thermodynamic restriction corresponding to Eq.(5) as a function of aspect ratios L/T and W/T. Constituent properties from Akiva et al. (1998)

Results for Eq. (5) are presented in Fig. 7 as one example of thermodynamic restriction that is not satisfied for all aspect ratios when Halpin-Tsai equations are considered.

Fig. 8 is a results summary of the dimension ranges that fulfill the thermodynamic restrictions. Combinations of aspect ratios that are not given in the ranges of Rubin et al. (2003) and this is indicated in the table by "out of range values".

It can be observed that only a small range of values satisfy simultaneously all thermodynamic restrictions when Halpin-Tsai equations are used. Therefore, these equations must be used with caution for the constituent properties given above.

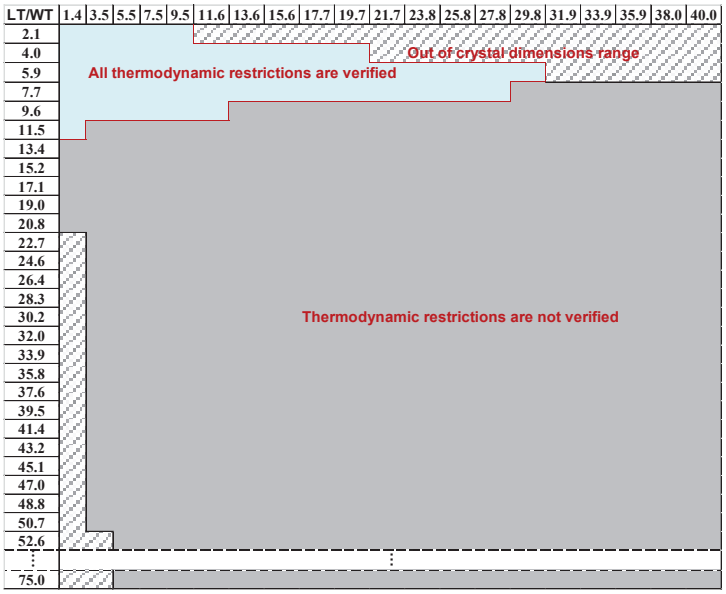

Fig. 8 Results summary for all thermodynamic restrictions when Halpin-Tsai equations are applied. $LT = L/T$ and $WT = W/T$. Constituent properties from Akiva et al. (1998)

5.2 Mineralized collagen fibril. Monoclinic homogenized stiffness matrix

We have calculated numerically the homogenized stiffness matrix of a mineralized collagen fibril using the finite element model described in Section 3. In order to perform comparisons with the recent models of Reisinger et al. (2011) in Section 6, collagen and mineral phases are assumed to be elastic isotropic as provided by these authors with Young's modulus $E_{col} = 5$ GPa (Cusak and Miller, 1979), $E_{ap} = 110.5$ GPa (Yao et al., 2007), and Poisson's ratios $\nu_{col} = 0.3$ and $\nu_{ap} = 0.28$ (Yao et al., 2007). As expected, results show a monoclinic behavior of the material because the staggered crystal pattern shows only one symmetry plane. The 3D homogenized stiffness matrix $\mathbf{C}^{fib}$ of

the mineralized collagen fibril for the case of $V_f = 0.3$ is:

$$\mathbf{C}_{fib} = \begin{pmatrix} 31.790 & 7.008 & 4.115 & 0 & 1.066 & 0 \\ & 25.050 & 3.666 & 0 & 0.162 & 0 \\ & & 9.706 & 0 & 0.001 & 0 \\ & & & 2.789 & 0 & 0.219 \\ & \text{sym} & & & 2.888 & 0 \\ & & & & & 7.745 \end{pmatrix} \text{GPa} \tag{14}$$

Considering the local orientated coordinate system $(1, 2, 3)$ shown in Fig. 1(b), the elastic constants for $V_f = 0.3$, can be calculated: $E_{11}^{fib} = 28.42$ GPa, $E_{22}^{fib} = 22.67$ GPa, $E_{33}^{fib} = 8.84$ GPa, $\nu_{12}^{fib} = 0.228$, $\nu_{23}^{fib} = 0.301$, $\nu_{31}^{fib} = 0.105$, $G_{12}^{fib} = 7.73$ GPa, $G_{23}^{fib} = 2.78$ GPa, $G_{31}^{fib} = 2.85$ GPa.

Similar analysis have been performed for other volume fractions. For $V_f = 0.1$, the Young's modulus in the longitudinal direction of the fibril is $E_{11}^{fib} = 9.1$ GPa whereas it increases to 43.87 GPa for $V_f = 0.45$.

Fig. 9 shows a deformed shape detail of the mineralized collagen fibril unit cell for each unitary strain field load case for the case $V_f = 0.3$.

The above results correspond to the local orientated coordinate system, as in Fig.1(b). For other values of ψ_1, ψ_2 the compliance matrix of the mineralized collagen fibril is calculated in the global coordinate system, $\mathbf{S}^g$, applying Lekhnitskii transformation for each sublayer of lamellar structure. In Figs. 10-11 it is shown the variation of Young's moduli of the fibril in the local auxiliary directions for a volume fraction $V_f = 0.3$.

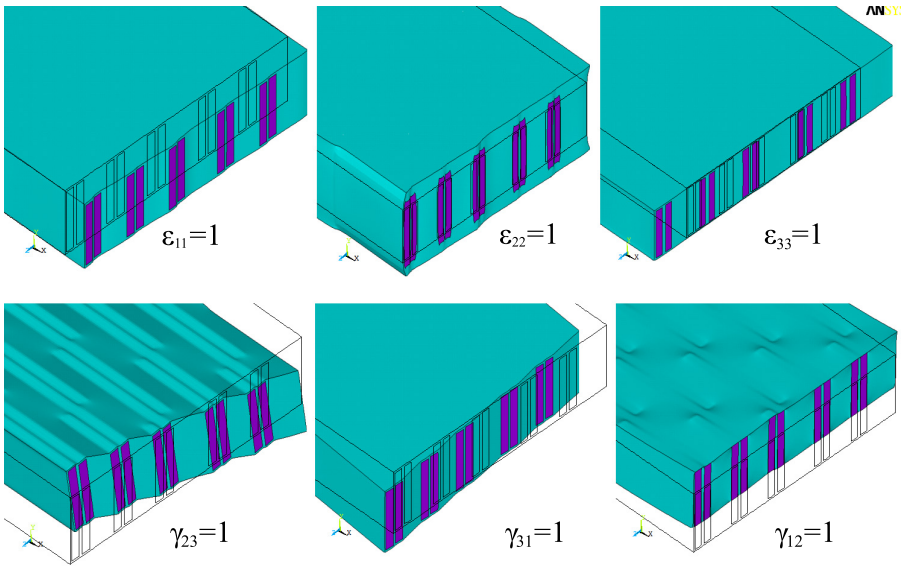

Fig. 9 Deformed shape detail of each unitary strain field, applied to calculate homogenized stiffness matrix of a mineralized collagen fibril, $V_f = 0.3$

Fig. 10 represents the variation of Young's modulus in x and y when angle ψ_1 takes values from 0° to 90°. In this case and since $\psi_2 = 0°$, the Young's modulus E^{fib}_{zz} is coincident with E^{fib}_{33} and remains with a constant value equal to 8.84 GPa. Note that E^{fib}_{yy} first decreases being its minimum value 20.54 GPa at about $\psi_1 = 40°$. E^{fib}_{xx} shows a complementary trend with respect to E^{fib}_{yy} being its minimum value at $\psi_1 = 50°$.

The trends for Poisson ratios and shear moduli are summarized next. The Poisson ratio that shows a greater variation with ψ_1 is ν^{fib}_{xy}, being its maximum value 0.346 at $\psi_1 = 40°$ and its minimum value 0.182 at $\psi_1 = 90°$. ν^{fib}_{yz} and ν^{fib}_{zx} present more uniform values being $\nu^{fib}_{yz}/\nu^{fib}_{zx} = [2.8 - 2.3]$ indicating a

high anisotropic behavior. Shear moduli G_{yz}^{fib} and G_{zx}^{fib} remain almost constant about 2.8 GPa. The maximum value is reached by G_{xy}^{fib}: 10.5 GPa at $\psi_1 = 45°$.

The Young's modulus of the mineralized collagen fibril as a function of the angle ψ_2 is shown in Fig. 11. Since $\psi_1 = 0$, the Young's modulus in x direction is constant, $E_{xx}^{fib} = 28.42$ GPa and is coincident with E_{11}^{fib}. Note that E_{zz}^{fib} first decreases with ψ_2 reaching the minimum value of 7.74 GPa at about $\psi_2 = 35°$. As expected, E_{yy}^{fib} shows a complementary trend with respect to E_{zz}^{fib}, being its minimum at about $\psi_2 = 55°$.

Poisson ratios and shear moduli variations with the angle ψ_2 have also been evaluated. The Poisson ratio ν_{xy}^{fib} does not vary much with ψ_2, taking values between 0.228 and 0.238. The greatest variation attained to ν_{yz}^{fib} from a maximum value of 0.493 at about $\psi_2 = 35°$ to a minimum value of 0.117 at $\psi_2 = 90°$. The variation of ν_{zx}^{fib} with the angle ψ_2 is similar to that shown with the angle ψ_1. All shear moduli vary widely with ψ_2. G_{xy}^{fib} and G_{zx}^{fib} show the same maximum value (7.73 GPa) at $\psi_2 = 0°$ and $90°$ respectively, showing also a symmetrical trend with respect to each other. G_{yz}^{fib} is maximum at $\psi_2 = 45°$ with 5.4 GPa.

5.3 5-layered lamella structure. Anisotropic homogenized stiffness matrix

Results show an anisotropic behavior of lamellar bone with a stiffness matrix with non-zero entries. The stiffness matrix $\mathbf{C}^{lam}$ has been calculated for different combinations of ψ_2 for the fourth and fifth layers and volume fraction $V_f = 0.3$. The stiffness matrix of lamellar bone, considering $\psi_2^{L4} = 70°$ and

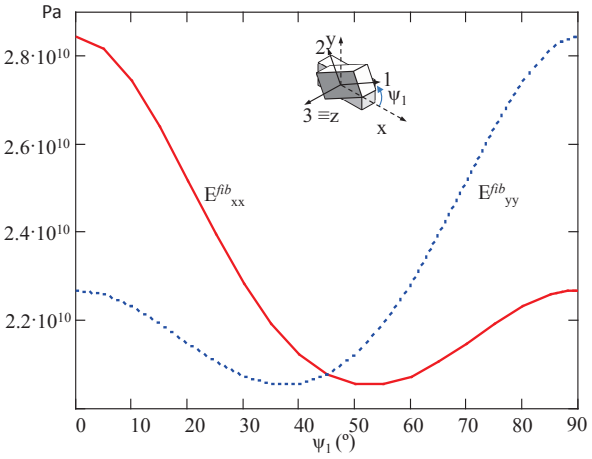

Fig. 10 Variation of mineralized collagen fibril Young's moduli $\left(E^{fib}_{xx}, E^{fib}_{yy}\right)$ in plane xy. ψ_1 is the rotation angle

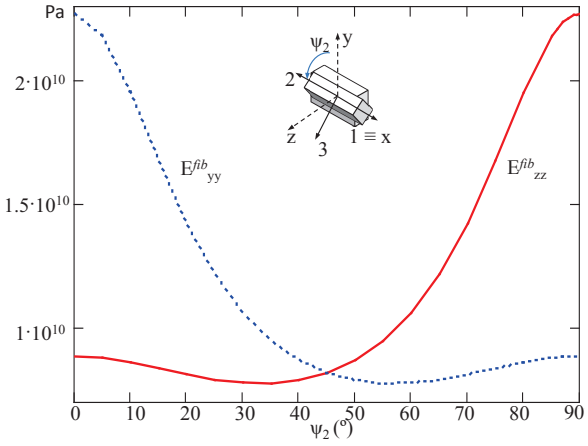

Fig. 11 Variation of mineralized collagen fibril Young's moduli $\left(E^{fib}_{yy}, E^{fib}_{zz}\right)$ in plane yz. ψ_2 is the rotation angle

$\psi_2^{L5} = 30°$, is:

$$\mathbf{C}_{lam} = \begin{pmatrix} 15.650 & 5.810 & 4.887 & -0.256 & -0.560 & -0.237 \\ & 28.960 & 5.061 & 0.194 & -0.372 & -0.169 \\ & & 13.830 & 0.272 & -1.816 & 0.266 \\ & & & 4.765 & -0.063 & 0.967 \\ & \text{sym} & & & 3.776 & -0.053 \\ & & & & & 5.541 \end{pmatrix} \text{GPa} \qquad (15)$$

Table 2 summarizes the elastic constants in the osteon coordinate system for several combinations of the angle ψ_2 of the fourth and fifth layers (superscripts $L4$ and $L5$ respectively).

It is important to note that the elastic constants are very influenced by ψ_2. Each elastic constant with superscript RM is obtained through rule-of-mixtures, Eq. (13). Results are expressed in the global osteon coordinate system, see Fig. 3. By comparing the rule-of-mixtures values with the ones calculated numerically, one can conclude that the rule-of-mixtures can be applied to obtain a preliminary estimation of the elastic constant properties. In general, both results obtained by finite element analysis and the rule-of-mixtures are in good agreement.

With the intention of quantify the influence of ψ_2 on the anisotropy of lamellar bone, Young's moduli have been calculated through the rule-of-mixtures as a function of of ψ_2^{L4} (see Fig. 12). The influence of the fourth layer is expected to be greater than the fifth layer because it is the thickest, and hence in

Table 2 *Elastic constants of lamellar bone using finite element analysis. Values with superscript RM are obtained using the rule-of-mixtures. Units of the Young's moduli and shear moduli are in GPa*

	$\psi_2^{L4}=0°$ $\psi_2^{L5}=0°$	$\psi_2^{L4}=50°$ $\psi_2^{L5}=90°$	$\psi_2^{L4}=70°$ $\psi_2^{L5}=90°$	$\psi_2^{L4}=70°$ $\psi_2^{L5}=30°$
E_{rr}	8.85	10.45	13.35	11.18
E_{rr}^{RM}	8.84	11.35	14.46	11.67
$E_{\theta\theta}$	23.04	12.50	12.62	13.29
$E_{\theta\theta}^{RM}$	22.91	12.18	12.32	13.05
E_{zz}	26.04	25.31	25.33	25.91
E_{zz}^{RM}	25.82	23.85	23.85	25.02
$\nu_{r\theta}$	0.114	0.286	0.256	0.255
$\nu_{r\theta}^{RM}$	0.114	0.351	0.330	0.331
$\nu_{\theta z}$	0.221	0.156	0.163	0.148
$\nu_{\theta z}^{RM}$	0.226	0.175	0.182	0.150
ν_{zr}	0.316	0.251	0.236	0.274
ν_{zr}^{RM}	0.314	0.247	0.228	0.279
$G_{r\theta}$	2.81	4.05	3.30	3.53
$G_{r\theta}^{RM}$	2.80	4.32	3.31	3.44
$G_{\theta z}$	8.40	5.59	5.15	5.34
$G_{\theta z}^{RM}$	8.32	5.15	4.71	5.03
G_{zr}	2.84	4.28	4.83	4.58
G_{zr}^{RM}	2.83	4.20	5.28	5.50

these analysis, ψ_2^{L5} has been fixed to 30°. As can be seen, the anisotropic behavior decreases when ψ_2^{L4} is large. For the analyzed case, $E_{rr}^{RM}=E_{\theta\theta}^{RM}=13.1$ GPa at $\psi_2^{L4}=75°$, while E_{zz}^{RM} remains constant as 25.02 GPa.

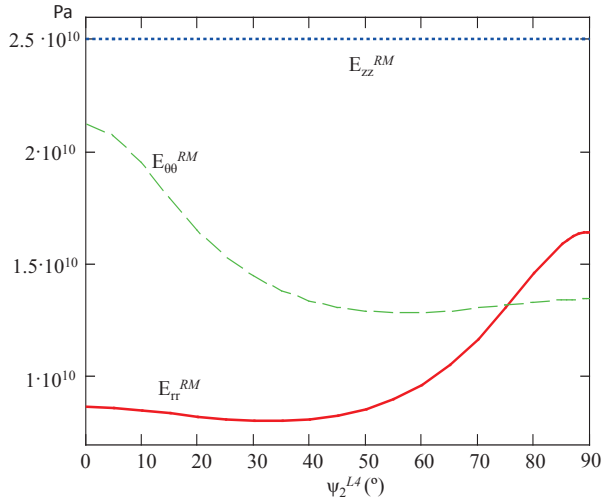

Fig. 12 Influence of ψ_2^{L4} on Young's moduli of lamellar bone calculated through the rule-of-mixtures. Note that $\psi_2^{L5} = 30°$ is fixed in order to analyze the influence of the thickest layer.

Fig. 13 shows the deformed shape of the 5-layered lamellar structure unit cell for the volume fraction $V_f = 0.3$. It has been checked that all stress components and deformed shapes of the unit cell are equal at opposite sides.

6 DISCUSSION AND CONCLUSIONS

As a result of the previous analysis, it can be concluded that careful attention must be paid if Halpin-Tsai equations are used to estimate the elastic constants of the mineralized collagen fibril. This is because not all possible dimensions of the crystal included in the ranges reported by (Rubin et al., 2003), lead to a positive definite stiffness matrix when using Halpin-Tsai equations with typical constituent properties, as those provided by Akiva et al. (1998).

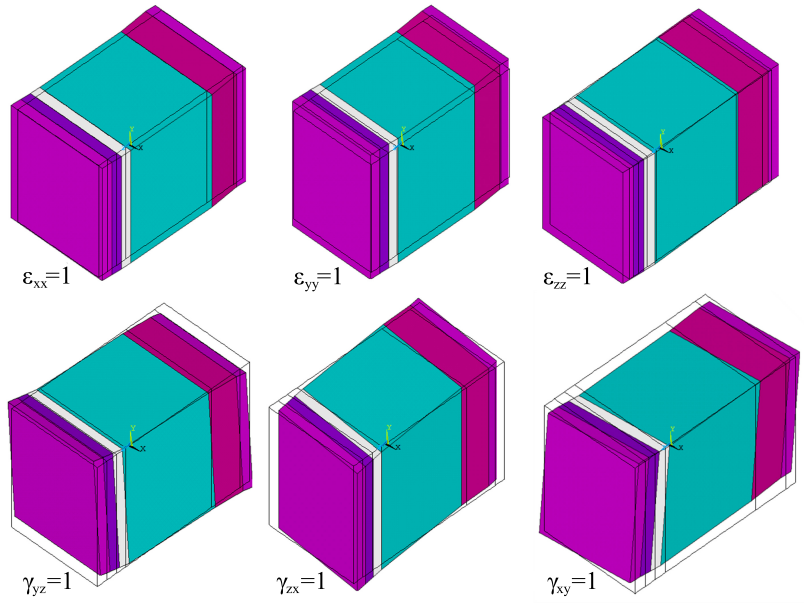

Fig. 13 Deformed shape detail of each unitary strain field, applied to calculate the homogenized stiffness matrix of lamellar bone. $V_f = 0.3$

A staggered arrangement of crystals is assumed in the fibril axial direction and parallel layers of crystals are considered in the fibril transverse direction. This model at sub-micro scale is based on the observation of previous investigators (Section 3.2). In this work, a monoclinic homogenized stiffness matrix of mineralized collagen fibril has been obtained numerically.

Elastic constants for a mineralized collagen fibril calculated in this work are not directly comparable with the ones obtained by Akiva et al. (1998). In the present work, other crystal dimensions and distance between crystals are considered and no assumption about material behavior is made. Akiva et al. (1998) use several theoretical models including Halpin-Tsai equations

despite the aspect ratios calculated with their crystal dimensions correspond to a non-positive definite stiffness matrix.

In this work, the 5-layer lamellar structure proposed by Weiner et al. (1999) has been also considered because it is in good agreement with the experimental results, following Reisinger et al. (2011). Since fibrils rotate in adjacent layers, the stiffness matrix exhibits an anisotropic behavior whose constants have been calculated.

The elastic constants of lamellar bone calculated in this work can be compared with values reported in the literature (see Table 3). Elastic constants for cortical bone of Cowin (1) are cited in Franzoso and Zysset (2009) and are summarized in this work. Yoon and Cowin (2008b) (2) and more recently Martínez-Reina et al. (2011) (3) use a complete analytical multiscale model where water content and porosity effects are included. Franzoso and Zysset (2009) (4) use nanoindentation techniques and Reisinger et al. (2011) (5) consider finite element models for different fibril patterns and homogenization theories to estimate fibril array elastic constants. Reisinger et al. (2011) assumed that crystals are spheroidal and randomly distributed in the collagen. This differs from the staggered arrangement of the crystal like platelets assumed in this work. The results of this work are given in column (6). These results correspond to the rotation angle $\psi_2 = 70^\circ$ and 30° for the sublayers fourth and fifth respectively. It can be seen that our results are in the range of reported values.

Table 3 *(1) Cowin (2001), (2) Yoon and Cowin (2008b), (3) Martínez-Reina et al. (2011), (4) Franzoso and Zysset (2009), (5) Reisinger et al. (2011), (6) this work, considering rotation angles* $\psi_2^{L4} = 70°$ *and* $\psi_2^{L5} = 30°$*. Units of Young's moduli and shear moduli are in GPa*

	(1)	(2)	(3)	(4)	(5)	(6)
E_{rr}	12.5	16.9	17.2	9.17± 0.63	16.3	11.18
$E_{\theta\theta}$	13	19.0	19.7	17.28± 1.89	17.5	13.29
E_{zz}	21	22.3	22.0	24.66± 2.71	24.0	25.91
$\nu_{r\theta}$	0.42			0.248± 0.012		0.255
$\nu_{\theta z}$	0.21			0.286± 0.024		0.148
ν_{zr}	0.33			0.557± 0.022		0.274
$G_{r\theta}$	4.45			4.69± 0.37		3.53
$G_{\theta z}$	5.3			7.68± 0.53		5.34
G_{zr}	5.8			5.61± 0.47		4.58

The homogenized stiffness matrix of lamellar bone is calculated using an analogous scheme as for mineralized collagen fibrils. Limitations of this model are the absence of water content, porosity and the extra-fibrilar matrix is also not considered. Future works could take into account these factors. In this work, a high influence of rotation angles ψ_1 and ψ_2 on the elastic constants estimation of lamellar bone has also been shown.

This study makes it possible to calculate the 3D stiffness matrix of the lamellar bone using the proposed numerical model, considering different rotation angles of the crystals in successive layers and different layer thicknesses. This contribution can be of interest for further 3D osteonal analysis.

Acknowledgements The authors acknowledge the Ministerio de Economía y Competitividad the financial support given through the project DPI2010-20990 and to the Programme Prometeo 2012/023. The authors thank Ms. Carla González Carrillo by her help in the development of some of the numerical models.

References

Akiva U, Wagner HD and Weiner S (1998) Modelling the three-dimensional elastic constants of parallel-fibred and lamellar bone. J Mater Sci 33:1497-1509

Ascenzi A, Bonucci E (1967) The tensile properties of single osteons. Anat Rec 158:375-386

Ascenzi A, Bonucci E (1968) The compressive properties of single osteons. Anat Rec 161:377-392

Ashman RB, Cowin SC, van Buskirk WC and Rice, JC (1984) A continuous wave technique for the measurement of the elastic properties of cortical bone. J Biomech 17:349-361

Bar-On B, Wagner HD (2012) Elastic modulus of hard tissues. J Biomech 45:672-678

Bondfield W and Li CH (1967) Anisotropy of nonelastic flow in bone. J Appl Phys 38:2450-

Cowin SC, van Buskirk WC (1986) Thermodynamic restrictions on the elastic constant of bone. J Biomech 19:85-86

Cowin SC (2001) Bone Mechanics Handbook, Second Edition. CRC Press Boca Raton, Florida.

Currey JD (1962) Strength of bone. Nature 195:513.

Currey JD (1975) The effect of stain rate, reconstruction and mineral content on some mechanical properties of bovine bone. J Biomech 12:313-319

Cusack S, Miller A (1979) Determination of the elastic constants of collagen by brillouin light scattering. J Mol Biol 135:39-51

Doty S, Robinson RA and Schofield B (1976) Morphology of bone and histochemical staining characteristics of bone cells. Handbook of Physiology, Ed Aurbach GD, American Physiology Soc, Washington DC 3-23

Erts D, Gathercole LJ ans Atkins EDT (1994) Scanning probe microscopy of crystallites in calcified collagen. J Mater Sci Mater Med 5:200-206

Faingold A, Sidney RC, Wagner HD (2012) Nanoindentation of osteonal bone lamellae. J Mech Biomech Materials 9:198-206

Franzoso G and Zysset PK (2009) Elastic anisotropy of human cortical bone secondary osteons measured by nanoindentation. J Biomech Eng 131:021001

Gebhardt W (1906) Arch Entw Mech Org 20:187-

Gibson RF (1994) Principles of composite material mechanics. McGraw-Hill

Gilmore RS and Katz JL (1982) Elastic properties of apatites. J Mater Sci 17:1131-1141

Giraud-Guille M (1988) Twisted plywood architecture of collagen fibrils in human compact bone osteons. Calcif Tissue Int 42:167-180

Gurtin ME (1972) The linear theory of elasticity. Handbuch del Physik VIa/2:1-296

Halpin JC (1984) Primer on Composite Materials: Analysis. Revised Edition. Technomic Publishing, Lancaster, PA

Hassenkam T, Fantner Ge, Cutroni JA, Weaver JC, Morse DE, Hanma PK (2004) High-resolution AFM imaging of intact and fractured trabecular bone. Bone 35:4-10

Hohe J (2003) A direct homogenization approach for determination of the stiffness matrix for microheterogeneous plates with application to sandwich panels. Composites Part B 34:615-626

Hulmes DJS, Wess TJ, Prockop DJ, Fratzl P (1995) Radial packing, order, and disorder in collagen fibrils. Biophys J 68:1661-1670

Jäger I, Fratzl P (2000) Mineralized collagen fibrils: a mechanical model with a staggered arrangement of mineral particles. Biophys J 79:1737-1746

Ji B, Gao H (2004) Mechanical properties of nanostructure of biological materials. J Mech Phy Sol 52:1963-1990

Landis WJ, Hodgens KJ, Aerna J, Song MJ, McEwen BF (1996) Structural relations between collagen and mineral in bone as determined by high voltage electron microscopic tomography. Microsc Res Tech 33:192-202

Lekhnitskii SG (1963) Theory of Elasticity of Anisotropic Elastic Body. Holden-Day, San Francisco, 1-73

Lempriere BM (1968) Poisson's ratio in orthotropic materials. Am Inst Aeronaut Astronaut J J6:2226-2227

Lowenstam HA, Weiner S (1989) On Biomineralization. Oxford University, New York

Lusis J, Woodhams RT and Xhantos M (1973). The effect of flake aspect ratio on flexural properties of mica reinforced plastics. Polym Engng Sci 13:139-145

Martínez-Reina J, Domínguez J, García-Aznar JM (2011) Effect of porosity and mineral content on the elastic constants of cortical bone: a multiscale approach. Biomech Model Mechanobiol 10:309-322

Orgel JPRO, Miller A, Irving TC, Fischetti RF, Hammersley AP, Wess TJ (2001) The in situ supermolecular structure of type I collagen. Structure 9:1061-1069

Padawer GE, Beecher N (1970) On the strength and stiffness of planar reinforced plastic resins. Polym Engng Sci 10:185-192

Pahr DH, Rammerstofer FG (2006) Buckling of honeycomb sandwiches: periodic finite element considerations. Comput Model Eng Sci 12:229-242

Reisinger AG, Pahr DH, Zysset PK (2010) Sensitivity analysis and parametric study of elastic properties of an unidirectional mineralized bone fibril-array using mean field methods. Biomech Model Mechanobiol 9:499-510

Reisinger AG, Pahr DH, Zysset PK (2011) Elastic anisotropy of bone lamellae as a function of fibril orientation pattern. Biomech Model Mechanobiol 10:67-77

Rezkinov N, Almany-Magal R, Shahar R and Weiner S (2013) Three-dimensional imaging of collagen fibril organization in rat circumferential

lamellar bone using a dual beam electron microscope reveals ordered and disordered sub-lamellar structures. Bone 52(2):676-683

Rho JY, Kuhn-Spearing L, Zioupos P (1998) Mechanical properties and the hierarchical structure of bone. Med Eng Phys 20:92-102

Rubin MA, Jasiuk I, Taylor J, Rubin J, Ganey T, Apkarian RP (2003) TEM analysis of the nanostructure of normal and osteoporotic human trabecular bone. Bone 33:270-282

Suquet P (1987) Lecture notes in physics-Homogenization techniques for composite media. Chapter IV. Springer, Berlin

Wagermaier W, Gupta HS, Gourrier A, Burghammer M, Roschger P, Fratzl P (2006) Spiral twisting of fiber orientation inside bone lamellae. Biointerphases 1:1-5

Wagner HD and Weiner S (1992) On the relationship between the microstructure of bone and its mechanical stiffness. J Biomech 25:1311-1320

Weiner S and Wagner HD (1998) The material bone: structure-mechanical funtion relations. Annu Rev Mater Sci 28:271-298

Weiner S, Traub W, Wagner H (1999) Lamellar bone: structure-function relations. J Struct Biol 126:241-255

Yao H, Ouyang L, Ching W (2007) Ab initio calculation of elastic constants of ceramic crystals. J Am Ceram 90:3194-3204

Yoon YJ, Cowin SC (2008b) The estimated elastic constants for a single bone osteonal lamella. Biomech Model Mechanobiol 7:1-11

Yuan F, Stock SR, Haeffner DR, Almer JD, Dunand DC, Brinson LC (2011) A new model to simulate the elastic properties of mineralized collagen fibril. Biomech Model Mechanobiol 10:147-160

Zhang Z, Zhang YWF and Gao H (2010) On optimal hierarchy of load-bearing biological materials. Proc R Soc B 278:519-525

Zuo S and Wei Y (2007) Effective elastic modulus of bone-like hierarchical materials. Acta Mechanica Solida Sinica 20:198-205